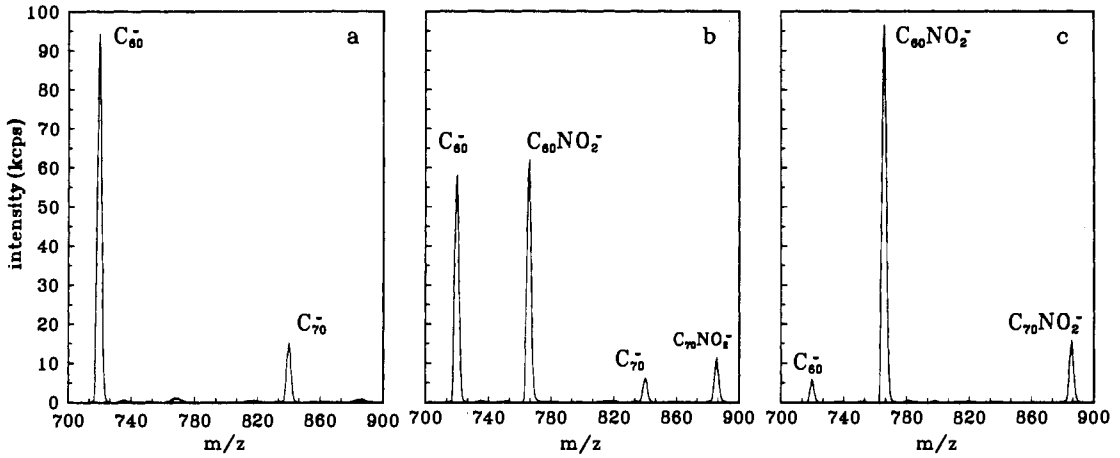

Figure 1. Mass spectra showing reactions of C_{60}^- and C_{70}^- with NO_2 at NO_2 flow rates (STP cm^3/min) of (a) 0.04, (b) 0.56, and (c) 2.6.

the 0.4 Torr of buffer gas in the flow tube can stabilize adducts through collisional cooling, this indicates that C_{60}^- and C_{70}^- do not form stable adducts with BF_3 and are therefore not Lewis bases.

C_{60}^- and C_{70}^- readily add NO_2 to form $C_{60}NO_2^-$ and $C_{70}NO_2^-$. Mass spectra for these reactions are shown in Figure 1. C_{60}^- is slightly less reactive than C_{70}^-. The rate constants measured in argon by using standard methods[8] are 1.2×10^{-10} cm^3/s and 2.1×10^{-10} cm^3/s, respectively, with error limits of ±40%. The relative error limits are much smaller, ca. 10%, so the ordering of reactivity is clear. For comparison, the collision rates for both reactions are estimated to be 6.4×10^{-10} cm^3/s.[9] The reactions are therefore 19% and 33% efficient, respectively. The structures of the adducts are unknown, with the nitro form ($C_nNO_2^-$) probably more stable and the nitrite form (C_nONO^-) possibly favored kinetically.[10] Further addition of NO_2 is at most very slow, with an apparent bimolecular rate constant of $\leq 10^{-13}$ cm^3/s. This shows that the first NO_2 addition deactivates the fullerides, at least with respect to further addition of NO_2. This suggests that the doublet character of the fullerides enhances reaction with NO_2, while $C_{60}NO_2^-$ and $C_{70}NO_2^-$, presumably singlets, are unreactive.

The apparent bimolecular rate constant for reaction with NO_2 is only weakly dependent on flow-tube pressure, with apparent rate constants for both fullerides at $P = 0.5$ Torr only slightly larger (ca. 50%) than the rate at 0.1 Torr. We interpret this to mean that adduct formation by termolecular association is nearly saturated at these flow-tube pressures.

NO_2 does not extract an electron from C_{60}^- or C_{70}^-, indicating that the vertical electron affinities of the corresponding fullerenes are greater than 2.27 eV,[11] the electron affinity (EA) of NO_2.[12] This is consistent with the work of Smalley and co-workers, who estimated EA(C_{60}) to be 2.6-2.8 eV from photoelectron measurements.[13] It is much greater than the EAs of polyaromatic hydrocarbons, which are typically in the range 0.5-1 eV. The high EAs for the fullerenes result from both their large size and the known effects of double-bond pyramidalization on electron binding energies (LUMO energies).[14]

C_{60}^- and C_{70}^- react with O_2 and NO in the flow tube slowly if at all, with effective bimolecular reaction rate coefficients of $<10^{-13}$ cm^3/s. By contrast, significant formation of neutral fullerene oxides in solution has been reported.[15] Since O_2 is a triplet and NO is a doublet, it is clear that simply having an unpaired electron is not sufficient to induce reactivity with gas-phase fullerides.

Acknowledgment. This work was supported by the National Science Foundation (CHE-8815502) and the Department of Energy, Office of Basic Energy Science. We thank Prof. R. G. Cooks for helpful comments.

(9) Calculated by using ADO theory: Su, T.; Bowers, M. T. In *Gas Phase Ion Chemistry*; Bowers, M. T., Ed.; Academic Press: New York, 1979; Vol. I, Chapter 3. $\mu_D(NO_2) = 0.316$ D taken from the following: Nelson, R. D.; Lide, D. R.; Maryott, A. A. *Natl. Stand. Ref. Data Ser. (U.S., Natl. Bur. Stand.)* **1967**, NSRDS-NBS 10. $\alpha(NO_2) = 3.02$ Å^3 taken from the following: Maryott, A. A.; Buckley, F. *Natl. Bur. Stand. Circ. (U.S.)* **1953**, *No. 537*.

(10) For examples of radical-ONO coupling, see: Bandow, H.; Akimoto, H.; Akiyama, S.; Tezuka, T. *Chem. Phys. Lett.* **1984**, *111*, 496-500 and references therein.

(11) Ervin, K. M.; Ho, J.; Lineberger, W. C. *J. Phys. Chem.* **1988**, *92*, 5405.

(12) The observation of both adduct formation and electron transfer in the analogous reaction of $C_5H_4^-$ with NO_2 suggests that competition from adduct formation does not prevent charge transfer. See: McDonald, R. N.; Chowdhury, A. K.; Setser, D. W. *J. Am. Chem. Soc.* **1980**, *102*, 6491-6498.

(13) Yang, S. H.; Pettiette, C. L.; Conceicao, J.; Chesnovsky, O.; Smalley, R. E. *Chem. Phys. Lett.* **1987**, *139*, 233-238.

(14) Stozier, R. W.; Caramella, P.; Houk, K. N. *J. Am. Chem. Soc.* **1979**, *101*, 1340-1343. Paddon-Row, M. N.; Rondan, N. G.; Houk, K. N.; Jordan, K. D. *J. Am. Chem. Soc.* **1982**, *104*, 1143. Borden, W. T. *Chem. Rev.* **1989**, *89*, 1095-1109. Chou, P. K.; Kass, S. R. *J. Am. Chem. Soc.* **1991**, *113*, 697-698.

(15) Wood, J. M.; Kahr, B.; Hoke, S. H.; Dejarme, L.; Cooks, R. G.; Ben-Amotz, D. *J. Am. Chem. Soc.*, in press.

Empirical Correlation between Protein Backbone Conformation and Cα and Cβ ^{13}C Nuclear Magnetic Resonance Chemical Shifts

Silvia Spera† and Ad Bax*

Laboratory of Chemical Physics, National Institute of Diabetes and Digestive and Kidney Diseases National Institutes of Health, Bethesda, Maryland 20892

Received February 27, 1991

For unstructured "random coil" peptides it has long been recognized that the chemical shift of the Cα and side-chain carbons of a given residue is largely independent of the nature of neighboring residues in the peptide, and "random coil" ^{13}C shifts have been reported for all amino acids.[1] In proteins, in contrast, widely different chemical shifts can be observed for a given type of amino acid. For example, Torchia et al.[2] reported a chemical shift distribution of over 8 ppm for the alanyl methyl carbons in staphylococcal nuclease (S.Nase). Previous solid-state NMR work suggested a strong correlation between peptide backbone conformation and ^{13}C chemical shifts. For a review, see Saito[3] and references therein. Theoretical FPT INDO calculations also predict different Cα and Cβ chemical shifts for helical and ex-

†On leave from Istituto Guido Donegani, Novara, Italy.

(1) Howarth, O. W.; Lilley, D. M. J. *Prog. NMR Spectrosc.* **1978**, *12*, 1-40.

(2) Torchia, D. A.; Sparks, S. W.; Bax, A. *Biochemistry* **1988**, *27*, 5135-5141.

(3) Saito, H. *Magn. Reson. Chem.* **1986**, *24*, 835-852.

0002-7863/91/1513-5490$02.50/0

tended structures,[4] although observed variations are significantly larger than the calculations predict.

Here we report an empirical correlation obtained for 442 residues for which the ϕ and ψ are known with good precision from high-resolution X-ray work. Our ^{13}C data base consists of four proteins for which complete ^{13}C chemical shift assignments are available: basic pancreatic trypsin inhibitor (BPTI),[5] calmodulin (CaM),[6] interleukin-1β (IL-1β),[7] and S.Nase.[8] The X-ray structures of these proteins have been solved at 1.0,[9] 2.2,[10] 2.0,[11] and 1.65 Å,[12] respectively. N- and C-terminal residues were excluded from the data base, as were residues for which no crystallographic coordinates were reported and residues that were of a different amino acid type in the crystallographic and NMR studies. Also excluded were regions with substantial disorder (i.e., large *B* factors), including part of the ω-loop of S.Nase (Glu43–Tyr54), residues Lys75–Ser81 of CaM, and eight residues of IL-1β for which the three available crystal structures[10] showed discrepancies in ϕ or ψ values of more than 30°. Histidine residues were excluded from our data base because their Cα and Cβ chemical shifts depend on the protonation state of the imidazole ring, which is not known exactly under the conditions (pH 5.8–7.4) where ^{13}C shifts were recorded. Cysteines involved in disulfide bridges were also excluded. A Ramachandran plot of the residues that make up our data base is shown in the supplementary material.

The deviation from random-coil chemical shift, often referred to as secondary shift, of residue k is referred to as $\delta(\phi_k,\psi_k)$, where ϕ_k and ψ_k are the dihedral backbone angles of residue k. The average value of $\delta(\phi_k,\psi_k)$, $\Delta(\phi,\psi)$, is shown in Figure 1, parts A (Cα) and B (Cβ). The $\Delta(\phi,\psi)$ surface is calculated from 442 $\delta(\phi_k,\psi_k)$ values from our data base (supplementary material). The rms deviation between measured $\delta(\phi_k,\psi_k)$ values and the $\Delta(\phi,\psi)$ surface was 1.10 ppm (Cα) and 1.14 ppm (Cβ). The rms deviation as a function of ϕ and ψ is shown in the supplementary material.

Figure 1C shows the distribution of secondary shifts in α-helix and β-sheet. In these histograms, all residues for which either the amide or the carbonyl (or both) is involved in an α-helical or antiparallel β-sheet type hydrogen bond are included except residues that have large deviations from the canonical backbone angles ($-90 < (\phi,\psi) < -10$ for α-helix and $-210 < \phi < -80$ and $90 < \psi < 200$). For α-helix (119 residues) the average Cα secondary shift is 3.09 ± 1.00 ppm and the average Cβ secondary shift is −0.38 ± 0.85 ppm. For β-sheet (126 residues), $\delta_{C\alpha} = -1.48 \pm 1.23$ and $\delta_{C\beta} = 2.16 \pm 1.91$ ppm. The larger rms spread for β-sheeted residues is largely caused by the fact that the ϕ and ψ angles of these residues show substantial variation ($\langle\phi\rangle = -114 \pm 32°$; $\langle\psi\rangle = 142 \pm 20°$) where 32° and 20° are the standard deviations. In α helices these angles have a much narrower distribution ($\langle\phi\rangle = -62 \pm 8°$; $\langle\psi\rangle = -42 \pm 10°$).

Although it may be tempting to use the secondary shift information for identifying regions of secondary structure, it should be noted that the basis of ^{13}C chemical shifts remains poorly

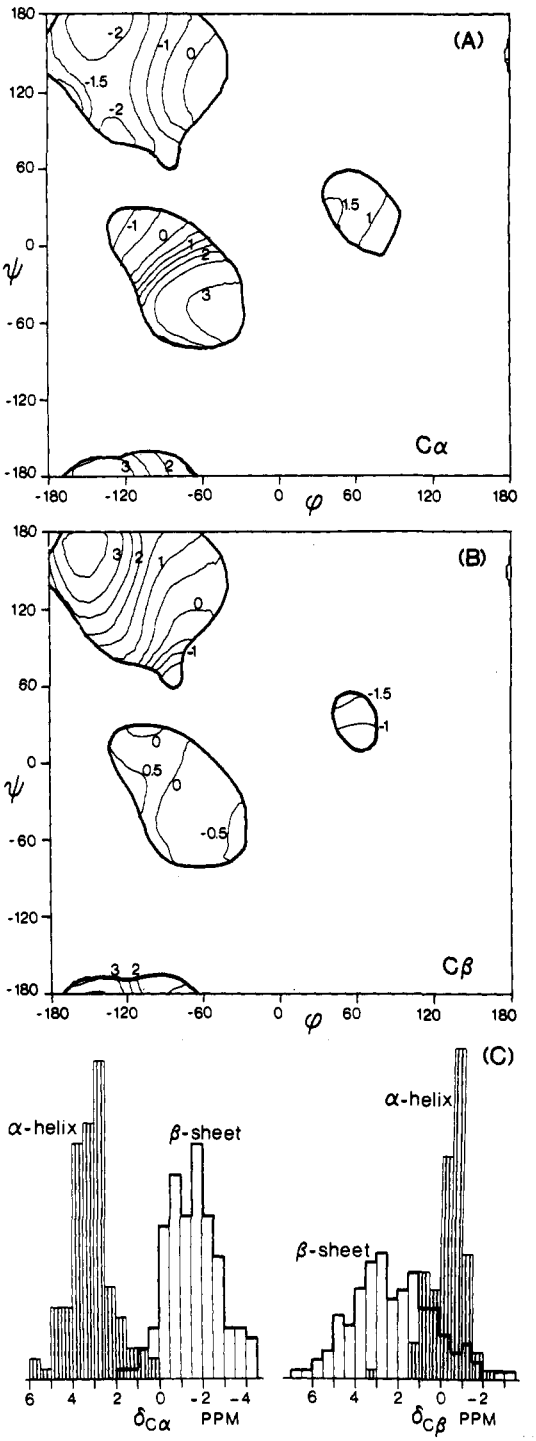

Figure 1. Contour plots of the average secondary shift, $\Delta(\phi,\psi)$, of (A) Cα and (B) Cβ resonances and (C) histograms of secondary shift distribution in α-helix and β-sheet. The $\Delta(\phi,\psi)$ surface is calculated by convolution of each of the $\delta(\phi_k,\psi_k)$ values with a Gaussian function, prior to addition and normalization: where the summations extend over all

$$\Delta(\phi,\psi) = \frac{\sum\delta(\phi_k,\psi_k)\exp(-((\phi-\phi_k)^2 + (\psi-\psi_k)^2)/450)}{\sum\exp(-((\phi-\phi_k)^2 + (\psi-\psi_k)^2)/450)}$$

residues k. Contours are only shown in regions of the ϕ,ψ plot where the residue density function, $\sum_k\exp(-((\phi-\phi_k)^2 + (\psi-\psi_k)^2)/450)$, is larger than 3.1, where the summation extends over all residues k. The data used for constructing Figure 1 are given in the supplementary material. Cα and Cβ random coil chemical shifts used for calculating the $\Delta(\phi,\psi)$ surfaces are as follows: Ala, 52.3, 19.0; Arg, 56.1, 30.3; Asn, 52.8, 37.9; Asp, 54.0, 40.8 (nonprotonated); Cys (reduced) 56.9, 28.9; Gln, 56.1, 28.4; Glu, 56.4, 29.7 (nonprotonated); Gly, 45.1; Ile, 61.3, 38.0; Leu, 55.1, 42.3; Lys, 56.5, 32.5; Met, 55.3, 32.6; Phe, 58.0, 39.0; Pro, 63.1, 31.7; Ser, 58.2, 63.2; Thr, 62.1, 69.2; Trp, 57.7, 30.3; Tyr, 58.1, 38.8; Val, 62.3, 32.1. Values are relative to internal TSP, where the 0 ppm ^{13}C frequency is obtained indirectly by multiplying the spectrometer frequency that corresponds to 0 ppm in the ^1H spectrum by 0.251 449 50.

(4) Ando, I.; Saito, H.; Tabeta, R.; Shoji, A.; Ozaki, T. *Macromolecules* **1984**, *17*, 457–461.
(5) (a) Wagner, A.; Bruehwiler, D. *Biochemistry* **1986**, *25*, 5939–5843 (because of a difference in referencing, 1.3 ppm was added to all reported shift values). (b) Hansen, P. E., submitted for publication.
(6) (a) Ikura, M.; Kay, L. E.; Bax, A. *Biochemistry* **1990**, *29*, 4659–4667. (b) Ikura, M.; Spera, S.; Barbato, N.; Kay, L. E.; Krinks, M.; Bax, A. *Biochemistry*, submitted.
(7) Clore, G. M.; Bax, A.; Driscoll, P. G.; Wingfield, P. T.; Gronenborn, A. M. *Biochemistry* **1990**, *29*, 8172–8184 (0.5 ppm was added to all shifts).
(8) Torchia, D. A., private communication.
(9) Wlodawer, A.; Deisenhofer, J.; Huber, R. *J. Mol. Biol.* **1987**, *193*, 145–156.
(10) Babu, Y. S.; Bugg, C. E.; Cook, W. J. *J. Mol. Biol.* **1988**, *204*, 191–204.
(11) (a) Finzel, B. C.; Clancy, L. L.; Holland, D. R.; Muchmore, S. W.; Watenpaugh, K. D.; Einspahr, H. M. *J. Mol. Biol.* **1989**, *209*, 779–791. (b) Priestle, J. P.; Schar, H. P.; Grutter, M. *Proc. Natl. Acad. Sci. U.S.A.* **1989**, *86*, 9667–9761. (c) Veerapandian, B.; Poulus, T. L.; Cilliland, G. L.; Anders Svensson, R. L.; Winborne, E. L.; Masui, Y.; Hirai, Y. Protein Brookhaven Data Bank No. 4I1B.
(12) Loll, P. J.; Lattman, E. E. *Proteins: Struct., Funct., Genet.* **1989**, *5*, 183–201.

understood and significant deviations from expected secondary shifts can occur (Figure 1C). The characteristic NOE patterns are the true markers defining regions of secondary structure in NMR studies of proteins. However, knowing the range in which Cα and Cβ carbons are expected to resonate, given that the secondary structure is known, greatly facilitates the spectral assignment process.

Our data base is too small for defining different $\Delta(\phi,\psi)$ functions for different amino acids, or for taking into account the side-chain conformations. However, we believe that the $\Delta(\phi,\psi)$ maps presented here facilitate spectral assignment for ^{13}C-enriched proteins. Cα and Cβ chemical shifts provide particularly promising structural probes for cases where other parameters such as ^1H–^1H NOE or J couplings cannot be measured, as is frequently the case for partially unfolded structures.

Acknowledgment. We thank Dennis Torchia, Donna Baldisseri, and Poul Hansen for making available to us the ^{13}C chemical shift data of S.Nase and BPTI, prior to publication. We are indebted to Mitsuhiko Ikura, Lewis Kay, Dennis Torchia, Marius Clore, Angela Gronenborn, and Ted Becker for substantial help and many useful and stimulating discussions. This work was supported by the AIDS Targeted Anti-Viral Program of the Office of the Director of the National Institutes of Health.

Supplementary Material Available: One figure showing the distribution of ϕ and ψ angles of the data base used, two figures showing the rms distribution of $\Delta(\phi,\psi)$ for Cα and Cβ, one table with all secondary shifts, and two tables with the secondary shifts for β-sheet and α-helix (15 pages). Ordering information is given on any current masthead page.

*Book Reviews**

Historical Atlas of Crystallography. Edited by J. Lima-de-Faria, with the collaboration of M. J. Buerger, J. P. Glusker, H. D. Megaw, P. B. Moore, M. Senechal, and W. A. Wooster. Kluwer Academic Publishers: Dordrecht, Holland. 1990. x + 158 pp. $36.00. ISBN 0-7923-0649-X.

This appealing book is the result of a cooperative effort by seven crystallographers, working under the auspices of the Commission of Crystallographic Teaching of the International Union of Crystallography.

The first 42 pages contain "time maps", the first one covering the development of crystallography as a whole over 5 centuries. This is followed by more detailed time maps of subfields: geometrical crystallography (19th and 20th centuries), physical, chemical crystallography, and crystal structure determination, all 20th century only. The time maps are chronologically arranged tables of entries characterizing each scientific advance or discovery. A collection of portraits and an extensive bibliography accompany the time maps.

The remainder of the volume contains articles on the history of each of the subfields, written by experts in each. These articles vary somewhat in technical depth, but for the most part the level of presentation does not require the reader to be an expert crystallographer. Of particular interest to chemists are the two chapters on the history of chemical crystallography, the chapter on inorganic compounds (Moore), and especially that on organic compounds (Glusker).

This book is warmly recommended to anyone with an interest in crystallography or in the history of science. Teachers of chemistry will find easy access to informative and interesting background material through applicable chapters in this book.

Christer E. Nordman, *University of Michigan*

Charged Particle Beams. By S. Humphries, Jr. (University of New Mexico). Wiley-Interscience: New York. 1990. xv + 834 pp. $145.00. ISBN 0-471-60014-8.

This is a book on high-energy beam physics put in 15 chapters. Chapter 1 gives the necessary definitions and reveals the organization of the book. Chapter 2 presents a very lucid introduction to the phase space theory and also treats charged particle dynamics, distribution functions, and numerical trajectory calculations. Chemists will perhaps miss SIMION (not even mentioned), while other trajectory-simulation codes (EGUN, PARAX5, WOLF) are used throughout the book. Beam optics is dealt with in Chapters 3 and 4; the topics covered include transformation methods, beam matching, nonlinear focusing systems, emittance in storage rings, and beam cooling. The next two chapters discuss in detail the space-charge effects (the Child law) and flow limitations derived thereof. The design and performance of high-current electron and ion guns and diodes are dealt with in Chapters 7 and 8. In the next chapter basic equations are derived for paraxial beam transport through cylindrical and quadrupole lenses. Chapter 10 deals with transport of high-current electron beams in solenoidal fields and magnetic cusps, including a discussion of interaction of fast electrons with matter. The techniques of positive ion beam neutralization by electron space charge are discussed in Chapter 11, while Chapter 12 in turn deals with electron beams in plasmas. Beam instabilities are treated in detail in Chapters 13 and 14. Finally, Chapter 15 deals with the generation and amplification of microwave radiation with electron beams in inverse diodes, klystrons, travelling-wave tubes, and magnetrons, including a brief discussion of the free-electron laser.

Although neither of these topics is likely to be discussed daily in an average chemistry laboratory, the book can make interesting reading for synchrotron users and those involved in electron and ion optics in general.

Frantisek Turecek, *University of Washington*

HPLC of Biological Macromolecules. Methods and Applications. Edited by K. M. Gooding (SynChrom, Inc.) and F. E. Regnier (Purdue University). Marcel Dekker, Inc.: New York and Basel. 1990. xiii + 680 pp. $150.00. ISBN 0-8247-7879-0.

Isolating a single active compound from the complex chemical milieu that is living tissue has always demanded the utmost from the chromatographic techniques used as well as in their skillful application. Biochemists as well as separation scientists were quick to adopt high-performance liquid chromatography (HPLC) as a tool. Unfortunately, communication between these two groups has, for the most part, been poor. This text represents a largely successful attempt to bridge the gap between these groups. However, this reviewer must offer one minor complaint before proceeding: although the title proclaims to encompass the HPLC of biological macromolecules, the text primarily focuses on the chromatography of proteins. Only about forty of the nearly seven hundred pages are devoted to nucleic acids; carbohydrates are essentially unmentioned except as glycoproteins.

The text is divided into three parts, the first being on individual chromatographic techniques, as well as on silica and organic supports, sample preparation, and gradient elution. Interestingly, affinity chromatography is absent in this section, as is any discussion of the chromatographic-like purifications being performed with cartridges. The second part describes the use of HPLC in the purification of various classes of polypeptides and proteins. Also included in this part are a chapter on the use of size exclusion chromatography for the measurement of protein–ligand and protein–protein interactions, as well as a chapter on the application of HPLC in the assay of enzymatic activities. The third part, really a single chapter, concerns the application of HPLC to the purification of oligonucleotides and tRNAs.

As with many multiauthored texts, there is a noticeable chapter-to-chapter variation in style. There is likewise a considerable variation in the depth of presentation. Some chapters in the first section (e.g., the chapters on silica, SEC, HIC, and sample preparation) are very nearly complete guides to the technique; others (e.g., the chapters on organic supports and IEC) are only surveys. The variation in the depth of presentation is reflected in the number of references: two chapters had only 8 references, including the chapter on IEC, while several chapters had more than one hundred references each. It is the responsibility of the editors to ensure uniformity of presentation. Further, there is also a significant amount of redundancy: several chapters in the second section each describe the fundamental modes of HPLC, operational considerations of each mode, etc., in spite of these modes being presented in detail in the first section. Again, the editors should have condensed these repetitions.

In spite of these short-comings, this is nonetheless a valuable text. In the preface, the editors state, "This book was written as a practical guide

*Unsigned book reviews are by the Book Review Editor.